Acta Mech 227, 743–756 (2016)
DOI 10.1007/s00707-015-1440-1

ORIGINAL PAPER

Junling Hou · Qun Li · Junnan Lv · Hong Zuo

Crack deflection by the transformable particles dispersed in composites

Received: 2 June 2015 / Revised: 7 July 2015 / Published online: 24 October 2015

Abstract The crack deflection in transformable particle-reinforced composites is studied in the present paper. The contribution of phase transformation on the crack tip J_k-integral ($k = 1, 2$) is explicitly determined by the material configurational theory. For the crack deflection angle from its original crack path induced by the phase transformation it can be shown that the crack initiates in the direction along which the potential energy release rate in terms of the crack tip J_k-integral possesses a stationary (maximum) value. The influence of one individual particle near the crack tip on the crack deflection is studied by accounting for both dilatant and shear transformation components. Furthermore, an FEM method is developed to model the stress-induced phase transformation on the basis of a macroscopic phenomenological constitutive model where multiple particles are taken to be non-uniformly distributed in a matrix. Numerical simulations are performed to observe the crack deflection by a cluster of particles. The results show a significant non-symmetric stress distribution locally at the crack tip, causing the crack to deflect. It is found that regions in the material with a higher volume fraction of transformable particles tend to deflect the crack growth more.

1 Introduction

It has been discovered that a second-phase constituent in the form of particles, ribbons, or fibers which undergoes a stress-induced phase transformation can be used to toughen composites [1–8]. Particularly, particle-reinforced composites have shown that the phase transformation from an austenitic phase to martensitic phase of particles dispersed in the matrix can give rise to a superelastic deformation which leads to substantial enhancements in tensile ductility and fracture toughness. A great effort has been made to explain the mechanisms of the transformation toughening in particle-reinforced composites [9–13]. One of the successful methods is the prediction of crack growth resistance for transformation-toughened materials in fracture terminology, for instance, the J-integral, the stress intensity factor, or the energy release rate near the crack tip. The role of transformation in toughening is examined within the context of the continuum theory by the extent to which the fracture parameter near the crack tip is altered by the transformation particles dispersed in composites. Moreover, it is of importance that the crack can be deflected from its original crack path due to the non-homogeneous material microstructure caused by the presence of particles. It is widely accepted that crack deflection can have a large influence on the toughness during crack growth, and the increase in fracture toughness can be explained by the crack deflection processes [14–19].

The main purpose of this study is to deal with the toughening mechanism of crack deflection due to the phase transformation combined of both dilatation and shear strain components for the non-homogeneous particle-reinforced materials where particles are not symmetric with respect to the crack surface. Attempts are

J. Hou · Q. Li (✉) · J. Lv · H. Zuo
State Key Laboratory for Strength and Vibration of Mechanical Structures, School of Aerospace,
Xi’an Jiaotong University, Xi’an 710049, China
E-mail: qunli@mail.xjtu.edu.cn

made to understand how a crack is deflected by transformable particles to the direction which is energetically more favorable. The contribution of phase transformation on the fracture toughness can be demonstrated by the material configurational forces associated with the J_k-integral. Recently, the configurational forces emerge as a strong tool to deal with crack problems associated with structural deformation, damage evolution, or phase transformation [20–22]. The significance of the material forces is indeed to deal with material inhomogeneity such as dislocations, cracks, inclusions, cavities, and non-homogeneities, which, under suitable conditions, can move or be displaced within the deformable material body in which they find themselves. In material space, the material forces are of specific interest as they are valuable to assess the failure of structures in the presence of defects. The material configurational theory seems to be an effective and reliable technique to provide an accurate result for crack deflection toughening induced by the transformable particles. In this study, the crack tip shielding can be estimated from the reduction in the crack tip J_k-integral compared with the remote J_k-integral. Herein, the component of J_1 is related to the driving forces as energy release rate for a crack advance along the crack direction, while the component of J_2 is the driving force for a crack deflection perpendicular to the crack surface. Consequently, a criterion is employed to predict the angle of crack deflection by assuming that the crack initiates in the direction along which the potential energy release rate in terms of the J_k-integral possesses a stationary (maximum) value. The present criterion is demonstrated to be effective in predicting the crack deflection and has a great advantage in dealing with crack deflection problems in non-homogeneous materials.

The present paper is organized as follows. First, the material configurational theory is constructed to analyze the crack deflection toughness by phase transformation in explicit form. The contribution of phase transformation has to be considered to evaluate the J_k-integral, and it leads to the conclusion that the crack tip J_k-integral is a more effective governing parameter than the remote J_k-integral. Second, we obtain the explicit solutions of the crack deflection by one individual particle embedded in a matrix with an edge crack. The increment of crack tip toughness associated with both dilatant and shear strains is also analyzed. Finally, numerical calculations are performed to observe the crack deflection behavior due to the stress-induced phase transformation which develops around the crack tip for the case of multiple particles. The finite element approach is employed based on the continuum constitutive model of the transformable bodies. Accurate constitutive models describing the toughening mechanism of the phase transformation have been well established [23–25]. In the simulations, a wake of fully transformed zone is considered near the crack tip leaving behind the crack when the stationary crack advances. In particular, we study the effect of clustered particles located in a specific local region on the crack deflection toughening in non-homogeneous composites by controlling the volume fraction of the transformation phase.

2 Fundamental solutions of crack deflection by phase transformation

The toughening mechanism due to the phase transformation accounting for both dilatation and shear strain can be investigated by the reduction in the fracture governing parameter, i.e., the J_k-integral near the crack tip. The present theoretical work is to extend the material configurational theory to obtain the contribution of the phase transformation to the J_k-integral in an explicit form.

A two-order material configurational stress tensor b_{ji} is introduced [26–29],

$$b_{ji} = W\delta_{ji} - \sigma_{jk}u_{k,i}. \tag{1}$$

Meanwhile, the material configurational forces are referred to by the term g_i, which originates from the material inhomogeneity:

$$g_i = -\left(\frac{\partial W}{\partial x_i}\right)_{\text{expl}}. \tag{2}$$

In Eqs. (1) and (2), W denotes the strain energy density of the elasticity system; δ_{ji} is the Kronecker delta whose value is 1 if the indices are equal, and 0 otherwise; σ_{jk} is the Cauchy stress tensor; $u_{k,i}$ are the first derivatives of the displacement; $(\partial W/\partial x_i)_{\text{expl}}$ denotes the explicit dependence of W on x_i. The physical interpretation of the configurational forces $b_{ji}(i, j = 1, 2)$ can be explained as the change in the total energy density at a point of an elastic continuum due to a material unit translation in x_j-direction of a unit surface with normal in x_i-direction [29].

An equilibrium equation between the configurational stresses b_{ji} and the configurational forces g_i can be established referring to Noether's theorem of certain conservation or balance laws, that is,

$$b_{ji,j} + g_i = 0. \tag{3}$$

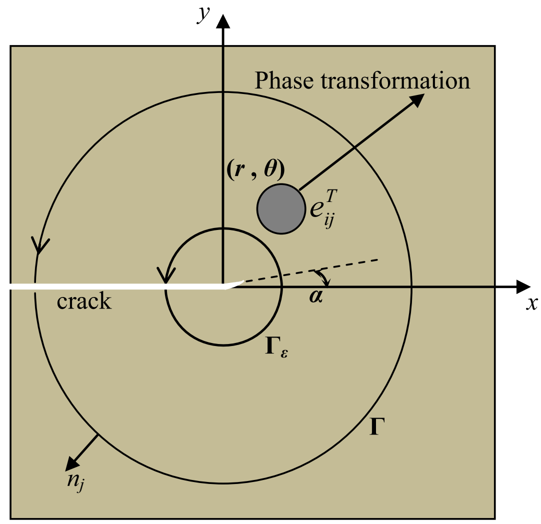

Fig. 1 Crack tip J_k-integral over the path Γ_ε only enclosing the crack tip; the remote J_k-integral over the path Γ enclosing all inhomogeneities including the phase transformable one and the crack tip; α is the deflection angle from its original crack path

The well-known J_k-integral in fracture mechanics can be formulated by the material configurational stresses Eq. (1) integrating over a path enclosing the crack tip [30–32],

$$J = J_1 = \oint_\Gamma b_{j1} n_j \mathrm{d}s = \oint_\Gamma (W n_1 - \sigma_{jk} u_{k,1} n_j)\mathrm{d}s, \tag{4}$$

$$J_2 = \oint_\Gamma b_{j2} n_j \mathrm{d}s = \oint_\Gamma (W n_2 - \sigma_{jk} u_{k,2} n_j)\mathrm{d}s, \tag{5}$$

where Γ is an integral contour beginning at the lower crack surface and ending at the upper surface and n_j refers to the outside normal of the contour Γ, as shown in Fig. 1.

For a single plane crack at the absence of phase transformation within the frame of linear elastic fracture mechanics, the J_k-integral has been related to potential energy releases associated with crack extension along the x_k-direction. It can be concluded that the path independence of the J_k-integral rigorously holds in such homogeneous materials. Additionally, one can conclude that the formulation of the J_k-integral calculated along the remote path Γ can be expressed in terms of the remote stress intensity factors [33]

$$J_{1\infty} = \frac{(K_{\mathrm{I}\infty}^2 + K_{\mathrm{II}\infty}^2)}{E'}, \qquad J_{2\infty} = -\frac{2K_{\mathrm{I}\infty} K_{\mathrm{II}\infty}}{E'} \tag{6}$$

with $E' = E$ for plane stress and $E' = E/(1-\nu^2)$ for plane strain, where E is the Young's modulus and ν is Poisson's ratio; the mode I and II stress intensity factors $K_{\mathrm{I}\infty}$ and $K_{\mathrm{II}\infty}$ depend on the remote loading and the geometric configuration [34].

In contrast to the J_k-integral in homogenous materials, we can conclude that the crack tip J_k-integral will lead to a set of quite different and intriguing features from those of the remote J_k-integral, i.e., an unexpected path dependence due to the contribution of material inhomogeneity such as transformable particles. Here, we define a fracture parameter, the $J_{k\mathrm{tip}}$-integral, computed around the crack tip along a vanishing small contour Γ_ε as shown in Fig. 1. Applying the divergence theorem for the contour $\Gamma - \Gamma_\varepsilon$ completely surrounding the region A and using the balance law of material configurational stresses in Eq. (3), one obtains

$$\begin{aligned} J_{k\mathrm{tip}} &= \lim_{\varepsilon \to 0} \int_{\Gamma_\varepsilon} b_{kj} n_j \mathrm{d}s = \int_\Gamma b_{kj} n_j \mathrm{d}s - \int_A b_{kj,j} \mathrm{d}A \\ &= \underbrace{\int_\Gamma \left(W\delta_{kj} - \sigma_{ij} u_{i,k}\right) n_j \mathrm{d}s}_{J_{k\infty}} + \underbrace{\int_A g_k \mathrm{d}A}_{G_k} \\ &= J_{k\infty} + G_k, \end{aligned} \tag{7}$$

where $J_{k\infty}$ denotes the remote J_k-integral in terms of the remote stress intensity factors as shown in Eq. (6); the configurational force g_k is defined as in Eq. (2); dA is the differential element of inhomogeneity; and G_k ($k = 1, 2$) denotes the total component of configurational forces given by integration of incremental value over the area of transformation zone A.

From Eq. (7), the term of configurational force in addition to the remote J_k-integral will contribute to the crack tip J_k-integral. In other words, there is a remarkable discrepancy between the crack tip J_k-integral and the remote J_k-integral and then the path dependence of the J_k-integral will appear attributing to the significant material configurational forces of the phase transformation. This path dependence of the J_k-integral as well as the contribution of phase transformation on the crack tip toughness suggests that the crack tip J_k-integral($J_{k\text{tip}}$) for a contour Γ_ε approaching zero radius around the crack tip is a more effective parameter to governing crack growth rather than the remote J_k-integral ($J_{k\infty}$). From Eq. (7), one can also conclude that the magnitude of the $J_{k\text{tip}}$-integral can be evaluated from the remote J_k-integral available in Eq. (6) and the configurational force g_k defined in Eq. (2) which can be analytically derived for some of specific problems as discussed in the next section.

Additionally, it is worth to note that the configurational force is related to the reduction in the crack tip $J_{k\text{tip}}$-integral compared with the remote $J_{k\infty}$-integral from Eq. (7), that is,

$$G_k = \Delta J_k = J_{k\text{tip}} - J_{k\infty}. \tag{8}$$

Thus, the configurational forces can be used to characterize the magnitude of transformation toughening due to the contribution of phase transformation. It should be mentioned that a negative value of configurational force denotes that the crack tip $J_{k\text{tip}}$-integral due to the presence of transformation is relaxed compared with the remote applied $J_{k\infty}$. Therefore, the phase transformation plays a role of the crack tip shielding. In contrast, a positive value of configurational forces denotes that the $J_{k\text{tip}}$-integral is enhanced comparing with $J_{k\infty}$, and hence, there is a crack tip anti-shielding effect due to phase transformation.

Moreover, the contribution of phase transformation can lead to the phenomenon that the crack propagation will be deflected from its original path due to a non-symmetric material structure with respect to the crack plane. Herein, a criterion to predict the crack deflection can be proposed according to the physical interpretation of the crack tip J_k-integral. The $J_{1\text{tip}}$-integral is identical to crack extension forces, and it has been given as the rate of total potential energy release per unit crack tip advance parallel to the crack direction. Analogously, the $J_{2\text{tip}}$-integral has been given a precise and clear physical significance as the rate of total energy release by postulating that the crack will skew and the tip advances perpendicular to the crack surface. Claiming that if the crack has advanced under an angle α with respect to its plane as depicted in Fig. 1, the energy release rate will be given by

$$G(\alpha) = J_{1\text{tip}} \cos\alpha + J_{2\text{tip}} \sin\alpha. \tag{9}$$

Therefore, the direction of crack deflection can be claimed such that the crack initiates in the direction along which the potential energy release $G(\alpha)$ possesses a stationary (maximum) value, i.e.,

$$\left.\frac{\partial G(\alpha)}{\partial\alpha}\right|_{\alpha=\alpha_0} = 0\,,\ \left.\frac{\partial^2 G(\alpha)}{\partial\alpha^2}\right|_{\alpha=\alpha_0} < 0. \tag{10}$$

It is well known that for a pure mode I crack in homogenous material where a negligible value of J_2 prevails, the crack will advance along the crack direction. In contrast, the introduction of phase transformation in the present study will result in the remarkable magnitude of J_2 near the crack tip. A mixed mode fracture can be characterized by the J_1- and J_2-integrals, and crack deflection will happen even under pure mode I loading. The theoretical framework given in this paper could provide a useful tool to deal with problems associated with the toughening and crack deflection mechanism of composites reinforced by transformable particles.

3 Crack deflection by one individual particle

The above analysis shows that the contribution of phase transformation on the crack deflection toughening can be analyzed in terms of the crack tip J_k-integral. In the following study, the explicit contribution of one individual transformable particle on the fracture toughening and crack deflection will be derived using an analytical method.

One individual, circular, transformable particle of radius R is assumed to locate at (r, θ) near the crack tip for a plane crack in brittle materials. Herein, the phase transformation strain is specialized as e_{ij}^T, where both dilatation and shear components are taken into account. The particle is assumed to be fully transformed, and the stress distribution inside the particle is uniform. The principle of linear superposition is adopted to determine the configurational forces due to the phase transformation [35,36].

The change in strain energy associated with the phase transformation can be given by

$$\mathrm{d}W = \sigma_{ij} e_{ij}^{T} \mathrm{d}A, \tag{11}$$

where σ_{ij} is the stress field near the crack tip in the absence of transformed particles under mixed mode I/II loadings, given by Westergaard [37]:

$$\begin{cases} \sigma_{11} = \frac{K_{\mathrm{I}}}{\sqrt{2\pi r}} \cos\frac{\theta}{2}\left(1 - \sin\frac{\theta}{2}\sin\frac{3\theta}{2}\right) - \frac{K_{\mathrm{II}}}{\sqrt{2\pi r}} \sin\frac{\theta}{2}\left(2 + \cos\frac{\theta}{2}\cos\frac{3\theta}{2}\right) \\ \sigma_{22} = \frac{K_{\mathrm{I}}}{\sqrt{2\pi r}} \cos\frac{\theta}{2}\left(1 + \sin\frac{\theta}{2}\sin\frac{3\theta}{2}\right) + \frac{K_{\mathrm{II}}}{\sqrt{2\pi r}} \sin\frac{\theta}{2}\cos\frac{\theta}{2}\cos\frac{3\theta}{2} \\ \sigma_{12} = \sigma_{21} = \frac{K_{\mathrm{I}}}{\sqrt{2\pi r}} \sin\frac{\theta}{2}\cos\frac{\theta}{2}\cos\frac{3\theta}{2} + \frac{K_{\mathrm{II}}}{\sqrt{2\pi r}} \cos\frac{\theta}{2}\left(1 - \sin\frac{\theta}{2}\sin\frac{3\theta}{2}\right) \end{cases} \tag{12}$$

According to Eqs. (2), (11), and (12), the total components of configurational forces over the particle can be computed by

$$\begin{aligned} G_x &= \Delta J_1 = \int_A g_x \mathrm{d}A \\ &= \pi R^2 \times \frac{r^{-3/2}}{4\sqrt{2\pi}} \begin{Bmatrix} \left[e_{11}^T\left(2\cos\frac{3\theta}{2} - 3\sin\theta\sin\frac{5\theta}{2}\right) + e_{22}^T\left(2\cos\frac{3\theta}{2} + 3\sin\theta\sin\frac{5\theta}{2}\right) + 6e_{12}^T\sin\theta\cos\frac{5\theta}{2}\right] K_I - \\ \left[e_{11}^T\left(4\sin\frac{3\theta}{2} + 3\sin\theta\cos\frac{5\theta}{2}\right) - 3e_{22}^T\sin\theta\cos\frac{5\theta}{2} + e_{12}^T\left(6\sin\theta\sin\frac{5\theta}{2} - 4\cos\frac{3\theta}{2}\right)\right] K_{II} \end{Bmatrix}, \\ G_y &= \Delta J_2 = \int_A g_y \mathrm{d}A \\ &= \pi R^2 \times \frac{r^{-3/2}}{4\sqrt{2\pi}} \begin{Bmatrix} \left[e_{11}^T\left(2\sin\frac{3\theta}{2} + \sin\frac{7\theta}{2} + \cos\theta\sin\frac{5\theta}{2}\right) + e_{22}^T\left(\sin\frac{3\theta}{2} + \cos\theta\sin\frac{5\theta}{2}\right) - 2e_{12}^T\left(\cos\theta\cos\frac{5\theta}{2} + \cos\frac{7\theta}{2}\right)\right] K_I + \\ \left[e_{11}^T\left(4\cos\frac{3\theta}{2} + \cos\frac{7\theta}{2} + \cos\theta\cos\frac{5\theta}{2}\right) - e_{22}^T\left(\cos\frac{7\theta}{2} + \cos\theta\cos\frac{5\theta}{2}\right) + e_{12}^T\left(4\sin\frac{3\theta}{2} + 2\sin\frac{7\theta}{2} + 2\cos\theta\sin\frac{5\theta}{2}\right)\right] K_{II} \end{Bmatrix}. \end{aligned} \tag{13}$$

Herein, one generally considers the phase transformation which involves a dilatation strain and a shear strain [17,18], that is,

$$e_{11}^T = e_{22}^T = e^T; \quad e_{12}^T = \lambda e^T, \tag{14}$$

where e^T denotes the dilatation strain and λ is the ratio between the transformation shear strain and dilatation strain.

Substituting (14) into Eq. (13), the crack tip J_k-integral disturbed by one transformable particle can be calculated by

$$\begin{aligned} G_x = \Delta J_1 = \pi R^2 e^T \times \frac{r^{-3/2}}{2\sqrt{2\pi}} &\left\{\left[2\cos\frac{3\theta}{2} + 3\lambda\sin\theta\cos\frac{5\theta}{2}\right] K_I \right. \\ &\left. - \left[2\sin\frac{3\theta}{2}\lambda + \left(3\sin\theta\sin\frac{5\theta}{2} - 2\cos\frac{3\theta}{2}\right)\right] K_{II}\right\}, \\ G_y = \Delta J_2 = \pi R^2 e^T \times \frac{r^{-3/2}}{2\sqrt{2\pi}} &\left\{\left[2\sin\frac{3\theta}{2} - \lambda\left(\cos\theta\cos\frac{5\theta}{2} + \cos\frac{7\theta}{2}\right)\right] K_I \right. \\ &\left. + \left[2\cos\frac{3\theta}{2} + \lambda\left(2\sin\frac{3\theta}{2} + \sin\frac{7\theta}{2} + \cos\theta\sin\frac{5\theta}{2}\right)\right] K_{II}\right\}. \end{aligned} \tag{15}$$

Meanwhile, the crack deflection angle can be formulated by the criterion of maximum energy release rate in Eqs. (9) and (10) by using Eqs. (6), (7) and (15), that is,

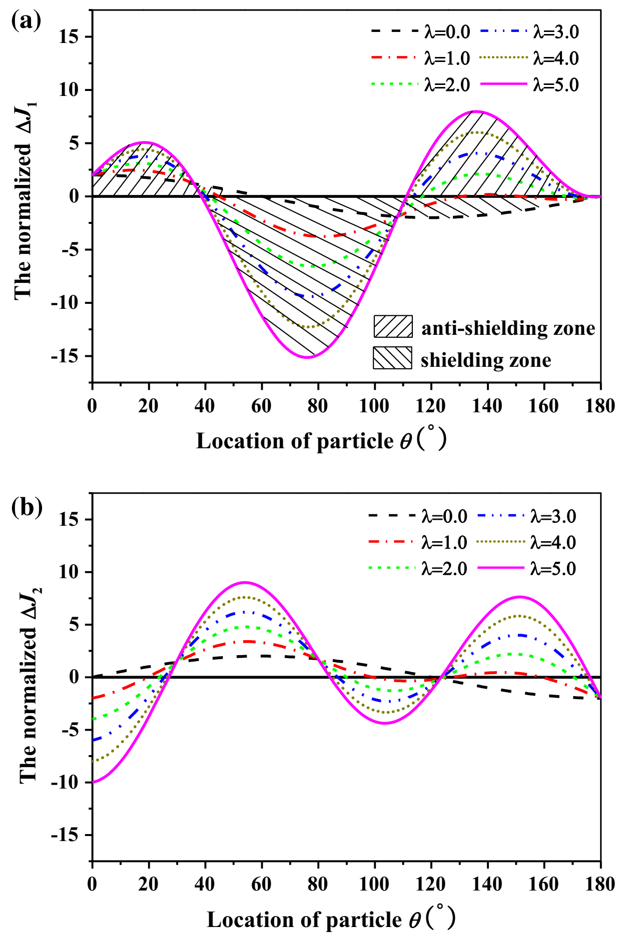

Fig. 2 Variable tendency of ΔJ_k against the location angle of one individual particle near the crack tip accounting for both shear strain and dilatation transformation strain. **a** $\triangle J_1$, **b** $\triangle J_2$

$$\alpha = \arctan\left(\frac{G_y + J_{2\infty}}{G_x + J_{1\infty}}\right)$$
$$= \arctan\left(\frac{E'\pi R^2 e^T \times r^{-3/2}\left\{\begin{array}{l}\left(2\sin\frac{3\theta}{2} - \lambda\cos\frac{7\theta}{2} - \lambda\cos\theta\cos\frac{5\theta}{2}\right)K_{I\infty} + \\ \left(2\lambda\sin\frac{3\theta}{2} + 2\cos\frac{3\theta}{2} + \lambda\sin\frac{7\theta}{2} + \lambda\cos\theta\sin\frac{5\theta}{2}\right)K_{II\infty}\end{array}\right\} - K_{I\infty}K_{II\infty}4\sqrt{2\pi}}{E'\pi R^2 e^T \times r^{-3/2}\left[\begin{array}{l}\left(2\cos\frac{3\theta}{2} + 3\lambda\sin\theta\cos\frac{5\theta}{2}\right)K_{I\infty} - \\ \left(2\sin\frac{3\theta}{2} - 2\lambda\cos\frac{3\theta}{2} + 3\lambda\sin\theta\sin\frac{5\theta}{2}\right)K_{II\infty}\end{array}\right] + (K_{\mathrm{I}\infty}^2 + K_{\mathrm{II}\infty}^2)2\sqrt{2\pi}}\right). \tag{16}$$

In order to clearly present the crack toughening by one transformable particle, numerical results of ΔJ_k representing the reduction in the crack tip J_k-integral compared with the remote J_k-integral are calculated from Eq. (15). The tendency of ΔJ_k normalized by $r_0^{-3/2} e^T \sqrt{\pi} R^2 K_{\mathrm{I}}$ against the variable location of particle is shown in Fig. 2 where the ratio of e_{12}^T / e^T changes from 0 to 5.0 and the specimen is subjected to the pure mode I loading. It becomes evident that the true $J_{k\mathrm{tip}}(k = 1)$-integral is an important fracture parameter governing the crack growth which is related to the released potential energy corresponding to the unit translation of crack tip along the crack direction. It can be concluded from Eq. (15) that the crack tip shielding or anti-shielding effect (i.e., the sign of ΔJ) will be dependent on the location angle of particle with respect to the crack face, and the ratio between the transformation shear and dilation strain, that is, $\Delta J_1 \propto 2\cos\frac{3\theta}{2} + 3\lambda\sin\theta\cos\frac{5\theta}{2}$. Particularly, the shielding or anti-shielding effect will be controlled by a function of $\cos\frac{3\theta}{2}$ for the pure dilatation

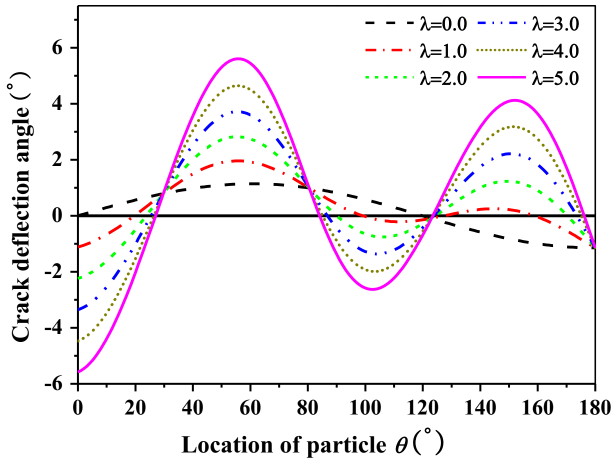

Fig. 3 Variable tendency of crack deflection angle from its original crack path against the location angle of one individual particle near the crack tip accounting for both shear strain and dilatation transformation strain

transformation and $\sin\theta\cos\frac{5\theta}{2}$ for the pure shear transformation. Figure 2a shows that there are some critical angles of crack tip shielding or anti-shielding by one single transformation particle undergoing a pure remote K_{I} loading at which the effect of transformed particle changes from the anti-shielding effect to shielding and vice versa. For instance, it can be shown that the particle has a shielding effect on the fracture toughness when the location angle of particle in the extent of (40°, 110°) for one zirconia (ZrO_2) particle with a shear strain of about 16% and a dilatation of 4% dispersed in composites as in Fig. 2a (λ= 4.0) [38].

In addition, Fig. 2b shows that a remarkable value of J_2 prevails for the crack at the presence of a transformable particle. This means that the crack will not advance along the crack direction. Crack deflection will happen due to the fact that the introduction of one particle results in the non-symmetric crack problem. The magnitude of crack deflection angle from its original crack path can be calculated by Eq. (16) under the remote mode I loading condition. It can be found from Eq. (16) that the value of the deflection angle is mainly determined by the relative value of configurational forces in the remote J_k-integral. A parametric study of G_k shows that its value depends on the size of the particle R, the location of the particle (r, θ) and the magnitude of the transformation strain (e^T, λ). Consequently, the amplitudes of the deviations from the original crack path will greatly depend on such parameters. Variable tendencies of crack deflection against the location of the transformable particle accounting for both dilatant and shear strain components are depicted in Fig. 3. It is seen that the deviation from the initial path is obvious which corresponds to an antisymmetric distribution of transformable phase relative to the crack surface. An obvious crack deflection can be found with the maximum magnitude of about 5.6° in the present analysis. The phenomenon can be useful to provide a theoretical reference for the investigation of crack deflection mechanism due to a stress-induced phase transformation with both dilatation and shear strain components.

4 Crack deflection by multiple particles

The above analysis presents the theoretical treatment of the influence of one transformable particle on the fracture toughening and crack deflection. The next study aims to investigate the crack deflection where the multiple particles are non-uniformly distributed in the matrix while a cluster of particles is aggregated in the local region. It has been reported that the stress-induced transformation in tetragonal zirconia can improve the toughness considerably due to the fact that the transformable particles are clustered in a duplex material consisting of a non-transformable alumina (Al_2O_3) matrix containing non-transformable tetragonal zirconia (t-ZrO_2) particles [14,15]. In the present study, a finite element approach is developed to obtain the stress and strain fields of a crack problem in particle-reinforced materials where the stress-induced phase transformation near the crack tip and the interaction between multiple particles are considered. Numerical results of the crack deflection from the original crack path are calculated, and the influence of non-homogeneous distribution of particles on the crack deflection is investigated.

Referring to the relevant finite element analysis, the material constitutive model by Auricchio [23–25] is proposed for stress-induced solid phase transformations. This constitutive model makes it possible to describe and interpret the various phenomena assuming that the particles undergo a phase transformation through austenite to martensite partially and then attain a steady state with the controlling of stress. Obviously, if the steady-state body is bearing a large enough loading, the dispersed particles whose parent phase is austenite would cause phase transformation.

Two of the phase transformations are considered here: austenite (A) → martensite (S) and S → A. Two internal variables, the martensite fraction (ξ_{S}) and the austenite fraction (ξ_{A}), are introduced. One of them is a dependent variable, and they are assumed to satisfy the relation

$$\xi_{\mathrm{S}} + \xi_{\mathrm{A}} = 1. \tag{17}$$

The independent internal variable chosen here is ξ_{S}.

Assuming that the material behavior to be isotropic, the pressure dependency of the phase transformation F is modeled by introducing the Drucker–Prager loading function, as follows:

$$\begin{aligned} F &= q + 3\beta p, \\ q &= \sqrt{\frac{3}{2}\mathbf{S} \times \mathbf{S}}, \\ \mathbf{S} &= \sigma - p\mathbf{1}, \\ p &= \frac{1}{3}\sigma \times \mathbf{1}, \end{aligned} \tag{18}$$

where $\mathbf{1}$ is the identity tensor, q, $\mathbf{S}$ denote the deviator stresses, p is the hydrostatic pressure, and β is the material parameter.

The evolution of the martensite fraction ξ_{S} is then defined as follows:

$$\dot{\xi}_s = \begin{cases} -H^{\mathrm{AS}}\left(1-\xi_{\mathrm{S}}\right)\frac{\dot{F}}{F-R_f^{\mathrm{AS}}} & \text{A} \rightarrow \text{S transformation,} \\ H^{\mathrm{SA}}\xi_{\mathrm{S}}\frac{\dot{F}}{F-R_f^{\mathrm{SA}}} & \text{S} \rightarrow \text{A transformation,} \end{cases} \tag{19}$$

where

$$\begin{cases} R_f^{\mathrm{AS}} = \sigma_f^{\mathrm{AS}}\left(1+\beta\right), \\ R_f^{\mathrm{SA}} = \sigma_f^{\mathrm{SA}}\left(1+\beta\right), \end{cases} \tag{20}$$

where σ_f^{AS} and σ_f^{SA} denote the final stress value for the forward phase transformation and the final stress value for the reverse phase transformation, respectively. And the value of H^{AS} and H^{SA} can be defined as follows:

$$H^{\mathrm{AS}} = \begin{cases} 1 & \text{if} \begin{cases} R_{\mathrm{S}}^{\mathrm{AS}} < F < R_f^{\mathrm{AS}} \\ \dot{F} > 0 \end{cases} \\ 0 & \text{otherwise} \end{cases} \tag{21}$$

$$H^{\mathrm{SA}} = \begin{cases} 1 & \text{if} \begin{cases} R_f^{\mathrm{SA}} < F < R_{\mathrm{S}}^{\mathrm{SA}} \\ \dot{F} < 0 \end{cases} \\ 0 & \text{otherwise} \end{cases} \tag{22}$$

where

$$\begin{cases} R_{\mathrm{S}}^{\mathrm{AS}} = \sigma_{\mathrm{S}}^{\mathrm{AS}}\left(1+\beta\right), \\ R_{\mathrm{S}}^{\mathrm{SA}} = \sigma_{\mathrm{S}}^{\mathrm{SA}}\left(1+\beta\right). \end{cases} \tag{23}$$

Then, the constitutive model is employed as

$$\begin{aligned} \sigma &= E \times \left(\varepsilon - \varepsilon_{tr}\right), \\ \dot{\varepsilon}_{tr} &= \dot{\xi}_{\mathrm{S}}\varepsilon_L\frac{\partial F}{\partial \sigma}, \end{aligned} \tag{24}$$

where E is the elastic stiffness tensor, ε is the total strain, ε_{tr} is the transformation strain tensor, and ε_L is the maximum residual strain.

Table 1 Material properties of transformable particles in numerical calculation [39]

E (GPa)	ν	σ_s^{AS} (MPa)	σ_f^{AS} (MPa)	σ_s^{SA} (MPa)	σ_f^{SA} (MPa)	ε_L	β
60	0.3	346	365	83	57	0.063	0.09

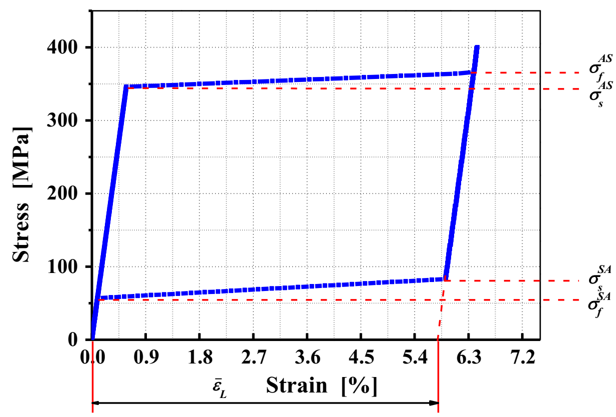

Fig. 4 Stress–strain relationship of phase transformation by FEM analysis

The material parameter β characterizes the material response in tension and compression. If tensile and compressive behaviors are the same, then $\beta = 0$. For a uniaxial tension–compression test, β can be related to the initial value of austenite to martensite phase transformation in tension and compression (σ_t^{SA} and σ_c^{SA}, respectively) as

$$\beta = \frac{\sigma_c^{\mathrm{AS}} - \sigma_t^{\mathrm{AS}}}{\sigma_c^{\mathrm{AS}} + \sigma_t^{\mathrm{AS}}}. \tag{25}$$

The material properties of transformable particle required for the present FEM analysis are determined from Favier et al. [39] and listed in Table 1. The matrix material is defined as an isotropic elastic material whose Young modulus $E_m = 29\,\mathrm{GPa}$ and the Possion's ratio $\nu = 0.33$. By FEM analysis, a typical stress–strain behavior for phase transformation is depicted in Fig. 4 in excess of the transformation stress.

To propose the present crack model for multiple transformable particles dispersed near the crack tip, it is essential to consider the notion of fully transformed zone. As is known, the phase transformation is triggered around the crack tip in the area where the local stress is assumed to be higher than the transformation critical values. The stress-induced transformable region can be subdivided into two parts due to the asymptotic stress distribution along the crack propagation direction [40]. One consists of a fully transformed zone and the other consists of a partially transformed zone, as depicted in Fig. 5a. The shape and size of the fully transformed zone can be determined approximately by the crack tip stress. The boundary of the fully transformed zone can be determined following Evans [1] and Yi and Gao [41]. The shape of the fully transformed zone is a long transformed wake which results from the steady-advanced propagation of the crack. As the crack advances under steady-state conditions, the transformation occurs along a curve in front of the crack tip leaving behind a semi-infinite wake of height $2H$. Thus, the boundary of the fully transformed zone for steady-advanced cracked material can be determined following Yi and Gao [41] as

$$r(\theta) = \begin{cases} H \times \dfrac{\cos^2\frac{\theta}{2}\left[1+3\sin^2\frac{\theta}{2}\right]}{\cos^2\frac{\hat{\theta}}{2}\left[1+3\sin^2\frac{\hat{\theta}}{2}\right]\sin\hat{\theta}} & 0 \le |\theta| \le \hat{\theta}, \\ \dfrac{H}{\sin(\theta)} & \hat{\theta} \le |\theta| \le \pi, \end{cases} \tag{26}$$

where $\widehat{\theta} = 82^\circ$ and

$$H = \frac{2}{\pi} \times \left[\frac{K_I}{\sigma_e^c(T,\xi)}\right]^2 \times \cos^2\frac{\hat{\theta}}{2}\left(1 + 3\sin^2\frac{\hat{\theta}}{2}\right)\sin\hat{\theta}. \tag{27}$$

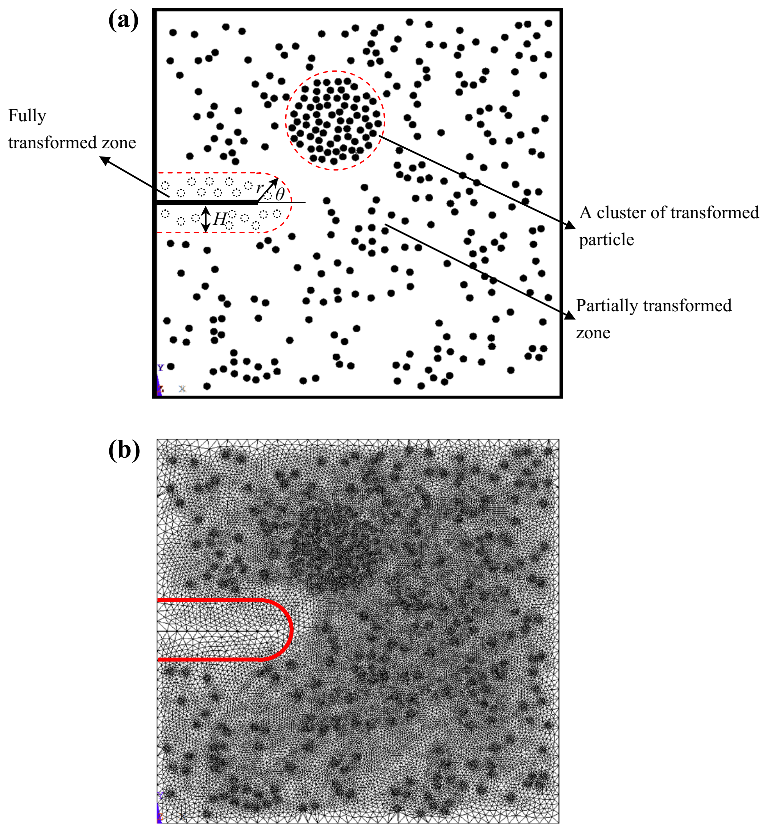

Fig. 5 Transformable particle-reinforced composites with full and partial phase transformation zone, and a cluster of transformed particles near the crack tip. **a** Schematic representation, **b** finite element mesh

In Eq. (27), σ_e^c is a parameter which depends on temperature T, chemical composition ξ, and material constants a, b, and g, and it is given by Sun and Hwang [42,43] and Fischer et al. [44] as

$$\sigma_e^c(T,\xi) = \frac{\sqrt{3}}{g}\left[(a+b\xi)(T-M_s)\right], \tag{28}$$

where M_s is the temperature of martensite start.

Considering the fully transformed zone and the partially transformed zone, Fig. 5b shows the finite element mesh where a cluster of particles is aggregated in a specific local zone and the distribution of transformed particles is non-symmetric with respect to the crack plane. The crack deflection angle is estimated by Eqs. (9) and (10), where the crack tip J_k-integral is numerically calculated by an equivalent domain integral method [45,46] in the fully transformed zone where the matrix is assumed to be homogenous, elastic. The integral contour to calculate the J_k-integral is only enclosing the crack tip without any particles to ensure the path-independence of the J_k-integral. The final results of the crack tip J_k-integral are obtained by an average over ten groups of random distributions for each case of volume fraction to reduce the errors from the specific random operation in numerical procedure. Figure 6 shows the numerically predicted crack deflection angle against the volume fraction of clustered particles near the crack tip where the tensile loading is large enough to ensure the transformation of most particles, especially in the clustered zone. The overall volume fraction of transformable particles is 5.0 %, while the local volume fracture of clustered zone changes from 25 to 50 %.

Despite the pure mode I loading, it should be reminded that a mixed mode fracture can be characterized by the J_1- and J_2-integrals for such a non-symmetric distribution of multiple particles around the propagating crack tip and thus crack deflection will happen. A magnitude of deflection angle about 5.1°–7.6° is expected as shown in Fig. 6. It can also be concluded that the present non-uniform distribution of the transformable phase leads to a positive deflection angle which means that the crack deflects upward from the original crack path. It means that crack meandering occurs around the crack face due to the fact that the region with higher transformable fraction seems to attract the crack. It is interesting to note that, as the volume fraction

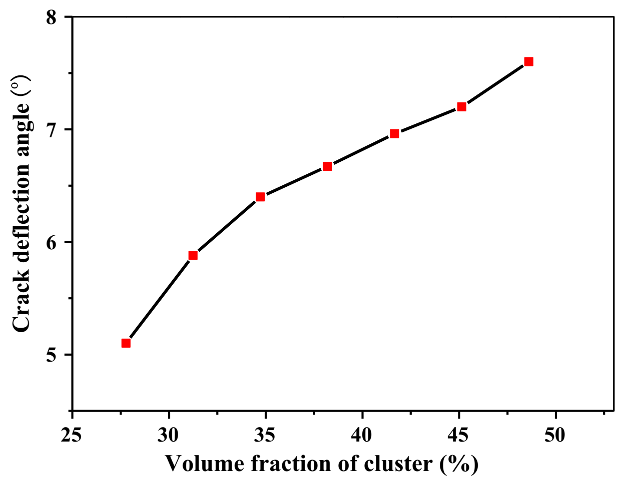

Fig. 6 Numerically predicted crack deflection angle against the volume fraction of clustered particles dispersed near the crack tip

of transformation increases, the deviation from the original crack path increases and the effect of attraction becomes stronger.

The phenomenon of crack deflection due to the transformation of dispersed particles can also be predicted and explained by the non-symmetric stress distribution around the crack tip. The equivalent stress distribution near the crack tip is calculated by the FEM approach as shown in Fig. 7. A strong non-symmetric stress distribution with respect to the crack surface is found in Fig. 7 as the transformable particle around the crack tip is non-symmetric with respect to the crack plane by a cluster of particles in non-homogeneous composites. In fact, we can derive the consistent conclusion by predicting the crack deflection according to the alternative method of the equivalent stress gradient criterion proposed by Zuo and Feng [47]. They assumed that the initial crack growth takes place in the direction along which the gradient of equivalent stress possesses a maximum value. From the stress distribution in Fig. 7, one can find an obvious non-symmetric gradient of equivalent stress which results in the crack deflection as predicted by the present maximum energy release in terms of the crack tip J_k-integral. The previous work by Zuo and Feng [47] predicted the crack growth by the gradient of equivalent stress. In contrast, the present failure criterion of potential energy release is associated with the J_k-integrals, which describes material's failure state from the view of energy. The failure criterion associated with the J_k-integral is the energetic treatment while the gradient of equivalent stress is the stress parameter approach. In other words, the present study is in the view of energy to get some indication of how crack deflects as the crack may find a path which is energetically more favorable.

5 Conclusions

Crack deflection is one of the most well-known toughening mechanisms in particle-reinforced transformable composites. The effect of transformable particles on the crack deflection is analyzed where both dilatation and shear transformation strain components are taken into account. The main conclusions are summarized as follows:

1. A general theory by the concept of material configurational forces is proposed to provide an effective method for investigating the fracture toughening and crack deflection occurring in the transformable material. The difference between the crack tip J_1-integral and the remote J_1-integral is used to estimate the crack shielding effect of phase transformation and the maximum energy release rate in terms of the crack tip J_k-integral to predict the crack deflection from its original crack path.
2. The contribution of one individual transformable particle on the crack deflection toughening is obtained in an explicit form. The most important conclusion from the analysis is that the crack tip shielding effect is mainly determined by the location angle of the particle with respect to the crack tip as well as the ratio between the shear and dilatation transformation strain components. Moreover, the crack deflection phenomenon is strongly dependent on the magnitude of shear and dilatation transformation strain, the location of the particle including the location angle, and the distance to the crack tip.

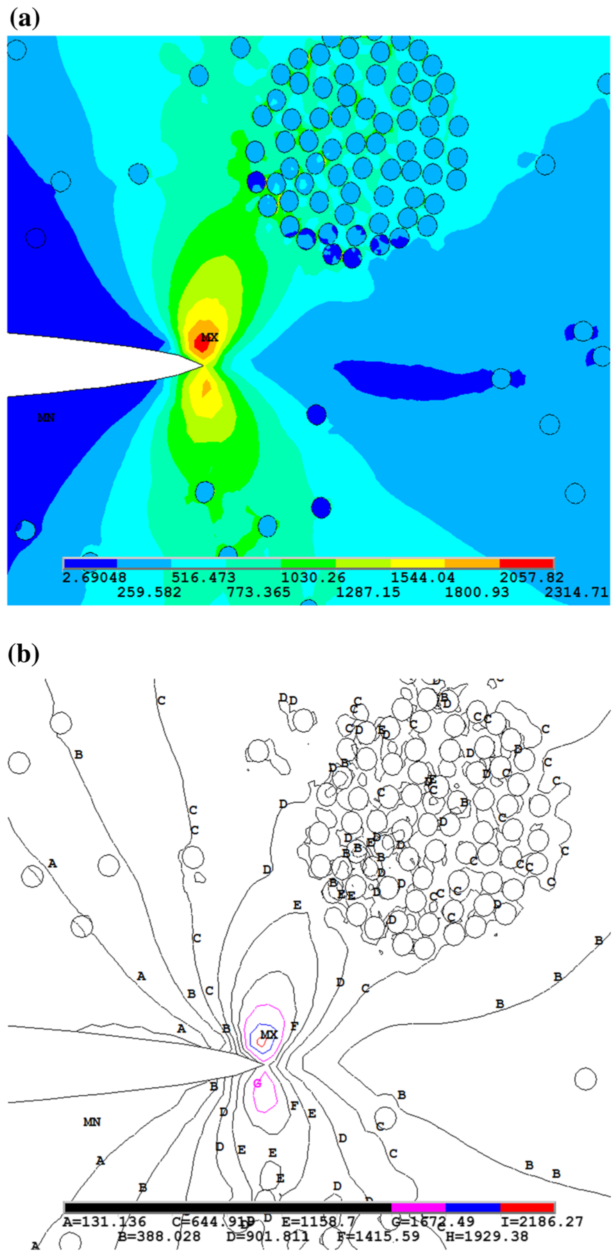

Fig. 7 Non-symmetric stress contour (**a**) and stress isohypses (**b**) with respect to the crack surface by a cluster of particles in non-homogeneous composites

3. A finite element approach is performed to solve the problem of multiple particles with non-uniform distribution embedded in composites. The crack deflection caused by a cluster of transformable particles has been discussed. It can be seen that the higher volume fraction of the cluster would cause a larger deflection angle with respect to the crack plane. The present theoretical and numerical study could be useful for dealing with problems which are focused on crack deflection influenced by the phase transformation in non-homogeneous composites.

Acknowledgments This work was supported by the National Natural Science Foundation of China with Grant Nos. 11472205, 11202156, 11321062, 11572235, and 11172228 and the Fundamental Research Funds for the Central Universities in China.

References

1. Evans, A.: Toughening mechanism in zirconia alloys. Adv. Ceram. **12**, 193–212 (1984)
2. Hutchison, J.W.: Mechanisms of toughening in ceramics. In: Theoretical and Applied Mechanics. Elsevier Science Publishers B.V. , North-Holland, IUTAM, pp. 139–144 (1989)
3. Shimamoto, A., Furuya, Y., Taya, M.: Active control of crack-tip stress intensity by contraction of shape memory TiNi fibers embedded in epoxy matrix composite. In: Intelligent Materials and Robots, 7th International Symposium, pp. 463–466 (1996)
4. Daly, S., Miller, A., Ravichandran, G., Bhattacharya, K.: An experimental investigation of crack initiation in thin sheets of nitinol. Acta Mater. **55**, 6322–6330 (2007)
5. Coughlin, J.P., Williams, J.J., Chawla, N.: Mechanical behavior of NiTi shape memory alloy fiber reinforced Sn matrix "smart" composites. J. Mater. Sci. **44**, 700–707 (2009)
6. Wang, S.B., Li, Y., Zhang, X.H.: Influence of the microstructure evolution of ZrO_2 fiber on the fracture toughness of ZrB_2–SiC nanocomposite ceramics. Mater. Des. **49**, 808–813 (2013)
7. Hu, J.Q., Zhang, Y., Liu, G., Wu, H.: Phase transformation behaviors of TiNi fibers embedded in an aluminum matrix. J. Alloys Compd. **589**, 491–497 (2014)
8. Barrett, R., Gross, R.S.: Super-active shape-memory alloy composites. Smart Mater. Struct. **5**, 255–260 (1996)
9. Claussen, N.: Fracture toughness of $A1_2O_3$ with an unstabilized ZrO_2 dispersed phase. J. Am. Ceram. Soc. **59**, 49–51 (1976)
10. Porter, D.L., Evans, A.G., Heuer, A.H.: Transformation-toughening in partially stabilized zirconia (PSZ). Acta Metall. **27**, 1649–1654 (1979)
11. Evans, A.G., Burlingame, N., Drory, M., Kriven, W.M.: Martensitic transformations in zirconia particle size effects and toughening. Acta Metall. **29**, 447–456 (1981)
12. Nakazawa, T., Funami, K., Wu, L.: Mechanical properties of Ti–Ni shape memory particle dispersed copper composite material. In: Chandra, T., Sakai, T. (ed.) Thermec '97—International Conference on Thermomechanical Processing of Steels and Other Materials, vol. **I**–**II**, pp. 1343–1349 (1997)
13. Danilenko, I., Glazunov, F., Konstantinova, T., Yashchyshyn, I., Burkhovetski, V., Volkova, G.: Effect of Ni/NiO particles on structure and crack propagation in zirconia based composites. Adv. Mat. Lett. **5**, 465–471 (2014)
14. Ruhle, M., Claussen, N., Heuer, A.H.: Transformation and microcrack toughening as complementary processes in ZrO_2-toughened Al_2O_3. J. Am. Ceram. Soc. **69**, 195–197 (1986)
15. Lutz, E.H., Claussen, N.: K^R-curve behavior of Duplex ceramics. J. Am. Ceram. Soc. **74**, 11–18 (1991)
16. Maugin, G.A.: Material Inhomogeneities in Elasticity. Chapman Hall, London (1993)
17. Stam, G.Th.M., van der Giessen, E.: Crack growth in non-homogeneous transformable ceramics. Part I: Constrained straight cracks. Int. J. Fract. **79**, 249–271 (1996a)
18. Stam, G.Th.M., van der Giessen, E.: Crack growth in non-homogeneous transformable ceramics. Part II: Crack deflection. Int. J. Fract. **79**, 273–293 (1996b)
19. Kienzler, R., Herrmann, G.: Mechanics of Material Space: With Applications to Defect and Fracture Mechanics. Springer, Berlin (2000)
20. Gurtin, M.E.: Configurational Forces as Basic Concepts of Continuum Physics. Springer, Berlin (2000)
21. Zhou, R., Li, Z., Sun, J.: Crack deflection and interface debonding in composite materials elucidated by the configuration force theory. Compos. Part B **42**, 1999–2003 (2011)
22. Li, Q, Lv, J.N., Hou, J.L., Zuo, H.: Crack-tip shielding by the dilatant transformation of particles/fibers embedded in composite materials. Theor. Appl. Fract. Mech. (2015). doi:10.1016/j.tafmec.2015.06.005
23. Auricchio, F., Taylor, R.L., Lubliner, J.: Shape-memory alloys: macro-modeling and numerical simulations of the superelastic behavior. Comput. Methods Appl. Mech. Eng. **146**, 281–312 (1997)
24. Auricchio, F., Petrini, L.: Improvements and algorithmical considerations on a recent three-dimensional model describing stress-induced solid phase transformations. Int. J. Numer. Method. Eng. **55**, 1255–1284 (2005)
25. Auricchio, F., Fugazza, D., DesRoches, R.: Numerical and experimental evaluation of the damping properties of shape-memory alloys. J. Eng. Mater. Tech. **128**, 312–319 (2006)
26. Kienzler, R., Herrmann, G.: On the properties of the Eshelby tensor. Acta Mech. **125**, 73–91 (1997)
27. Budiansky, B., Rice, J.R.: Conservation laws and energy release rates. J. Appl. Mech. **40**, 201–203 (1973)
28. Eshelby, J.D.: The elastic energy-momentum tensor. J. Elast. **5**, 321–335 (1975)
29. Herrmann, A.G., Herrmann, G.: On energy-release rates for a plane crack. J. Appl. Mech. **48**, 525–528 (1981)
30. Chen, Y.H.: Advances in Conservation Laws and Energy Release Rates. Kluwer Academic Publishers, The Netherlands (2002)
31. Cherepanov, G.P.: The propagation of cracks in a continuous medium. J. Appl. Math. Mech. **31**, 503–512 (1967)
32. Rice, J.R.: A path independent integral and the approximate analysis of strain concentration by notch and cracks. J. Appl. Mech. **35**, 379–386 (1968)
33. Liebowitz, H.: Fracture: An Advanced Treatise. Academic Press, New York (1969)
34. Irwin, G.R.: Analysis of stresses and strains near the end of a crack traversing a plate. J. Appl. Mech. **24**, 361–364 (1957)
35. McMeeking, R.M., Evans, A.G.: Mechanics of transformation toughening in brittle materials. J. Am. Ceram. Soc. **65**, 242–246 (1982)
36. Li, Z.H., Yang, L.H.: The near-tip stress intensity factors for a short crack partially penetrating an inclusion. J. Appl. Mech. **71**, 465–469 (2004)
37. Westergaard, H.M.: Stresses at a crack, size of the crack and the bending of reinforced concrete. Proc. Am. Concr. Inst. **30**, 93–102 (1934)
38. Budiansky, B., Hutchinson, J.W., Lambropoulos, J.C.: Continuum theory of dilatant transformation toughening in ceramics. Int. J. Solids Struct. **19**, 337–355 (1983)
39. Favier, D., Liu, Y., Orgeas, L. et al.: Influence of thermomechanical processing on the superelastic properties of a Ni-rich nitinol shape memory alloy. Mater. Sci. Eng. A **429**, 130–136 (2006)

40. Xiong, F., Liu, Y.: Effect of stress-induced martensitic transformation on the crack tip stress-intensity factor in Ni–Mn–Ga shape memory alloy. Acta Mater. **55**, 5621–5629 (2007)
41. Yi, S., Gao, S.: Fracture toughening mechanism of shape memory alloys due to martensite transformation. Int. J. Solids Struct. **37**, 5315–5327 (2000)
42. Sun, Q., Hwang, K.: Micromechanics modeling for the constitutive behavior of polycrystalline shape memory alloys. J. Mech. Phys. Solids **41**, 1–19 (1993a)
43. Sun, Q., Hwang, K.: Micromechanics modeling for the constitutive behavior of polycrystalline shape memory alloys. J. Mech. Phys. Solids **41**, 20–33 (1993a)
44. Fischer, F., Sun, Q., Tanaka, K.: Transformation-induced plasticity (TRIP). Appl. Mech. Rev. **49**, 31–364 (1996)
45. Moura, B., Shih, C.F.: A treatment of crack tip contour integrals. Int. J. Fract. **35**, 295–310 (1987)
46. Shivakumar, K.N., Raju, I.S.: An equivalent domain integral method for three-dimensional mixed-mode fracture problem. Eng. Fract. Mech. **42**, 935–959 (1992)
47. Zuo, H., Feng, Y.H.: A universal crack extension criterion based on the equivalent stress gradient: I. Theory and numerical verification. Acta Mech. Solida Sin. **25**, 100–110 (2012)